A BRIEF HISTORY OF FRACTOGRAPHY

S. P. Lynch[+]* and S. Moutsos*
*Monash University, Clayton Vic. 3168 Australia, [+] DSTO, Fishermans Bend, Vic. 3207 Australia

ABSTRACT

Fracture surfaces have, no doubt, been studied throughout the history of mankind, probably starting with observations on stone-age tools. In the 16-18th centuries, the macroscopic appearance of fracture surfaces was used to assess the quality of metallic materials, with studies by Réaumur in 1722 being the most notable. However, it was not until 1943 that fracture surfaces were first examined at high-magnifications (using optical microscopy up to 1,000x), and that the first attempts were made to examine replicas of fracture surfaces using transmission-electron microscopy (TEM). Early replicas had poor fidelity and resolution, and it was not until 1956 that Crussard et al. pioneered high-resolution TEM fractography using shadowed, direct-carbon replicas. This technique (and its subsequent variations) revolutionised fractography and led to a plethora of studies in the 1960's and 70's. It therefore seems appropriate to commemorate the 50th anniversary of high-resolution electron fractography with a review of how it, and subsequent scanning electron microscopy (SEM) and other techniques, have led to a better understanding of fracture processes. Such understanding has been invaluable in failure analysis and in developing improved materials. Milestone observations for a number of important modes of fracture in inert environments including cleavage, brittle intergranular fracture, dimpled overload fractures, and fatigue fractures, are described first, followed by examples of key observations for fractures produced in embrittling environments.

Overload Fracture by Cleavage

Cleavage of minerals had probably been noted in early times, but the first significant scientific observations appear to have been made by Guglielmini (1688) and subsequently by Haüy (1784), who noted that the cleavage always occurred on the same plane, with Haüy producing rhombohedral crystals of calcite by cleavage regardless of the external shape of the crystals [1]. In the sixteenth to eighteenth centuries, numerous examples of the use of fracture-surface appearance to assess both the quality of metals and the effects of alloying elements were reported. Fractures exhibiting smooth and bright planes, i.e. cleavage (or brittle intergranular) facets, were recognized as indicative of poor quality. The most comprehensive of these early fractographic studies was by Réaumur (1722) who described seven classes of iron according to their fracture-surface appearance. The first type exhibited "….very brilliant white platelets, which appear to be as many little mirrors of irregular shape and arrangement…" – a nice description of cleavage in polycrystals (Fig.1) [2, 3] #. In the mid-to-late nineteenth century, observations that large grains of iron alloys could be cleaved to produce small cubes [4] (like the much earlier observations for minerals) strongly supported the case that metals were also crystalline – a view that was then not universally accepted.

The first detailed studies of cleavage fractures at high magnifications, showing a wealth of detail, were published in 1943 by Zappfe and Moore [5], and then in 1945 by Zappfe and Clogg [6] who used the term 'fractography' for the first time. They showed, for example, that {100} fractures in an iron-silicon alloy exhibited river lines (converging steps parallel to the direction of crack growth), tongues (where twins had formed ahead of cracks with subsequent crack growth along the twin-matrix interface), and slight tilts across sub-grain boundaries (Fig. 2). Hull and Beardmore [7] subsequently showed that river lines on {100} cleavage planes occurred preferentially on <110> directions. Examination of cleavage fracture surfaces using TEM by Crussard and his colleagues [8] in 1956 and subsequently by Beachem [9], Henry and Plateau [10], and others, revealed finer steps and tongues than detected by optical microscopy, and indicated that areas between these features were featureless even at high magnifications (Fig. 3). Recent scanning-tunnelling microscopy (STM) of cleaved chromium single crystals has shown that fractures can be atomically flat between atomic-scale steps (Fig. 4) [11].

The preference for cleavage on {100} planes in <110> directions for bcc metals is somewhat surprising since Griffith's thermodynamic surface-energy criterion for brittle fracture (1921)[12] predicts that (i) the favoured cleavage plane (for elastically isotropic metals) should be the {110} plane which has the minimum surface energy, and (ii) there should be no preferred direction. Etch pits on cleavage fracture surfaces, and other observations, show that some dislocation activity

These references describe the early history of fractography in detail, show other examples of sketches by Réaumur , and provide original references of early studies. Also note that micrographs from the literature have been cropped to save space, and clearer scale bars and other annotations have been added.

accompanies cleavage, and it has been suggested that preferred cleavage planes and directions are those for which the extent of plasticity around cracks is minimised. More recent work [13] suggests that cleavage anisotropy may be intrinsic and associated with 'lattice-trapping'. For example, the cleavage (decohesion) process could involve incipient (reversible) dislocation emission at crack tips [14], i.e. shear plus tensile displacements of atoms at crack tips rather than just tensile separation of atoms, which would be facilitated if crack fronts were along <110> directions – the line of intersection of crack planes and slip planes. For the {100} plane, there would be two easy <110> directions for cleavage whereas there would be only one such direction for the {110} plane – which might explain why {100} planes are often favoured.

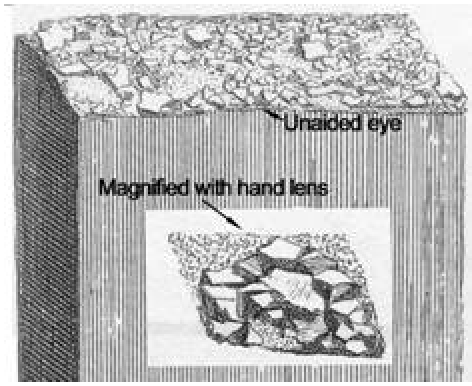

Figure 1. Sketches by Réaumur (1722) of cleavage fracture of polycrystalline iron, described as "… little mirrors of irregular shape and arrangement'' [2, 3].

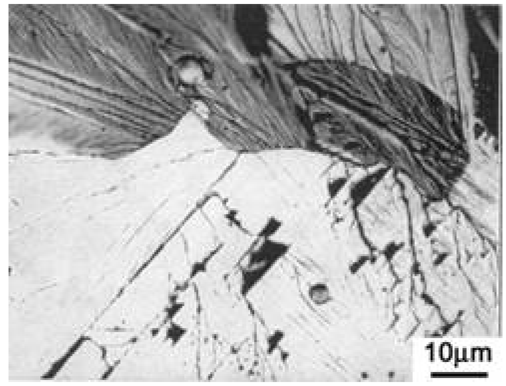

Figure 2. Optical fractography of a {100} cleavage fracture surface of an Fe-Si alloy, exhibiting river lines, tongues, and sub-grain boundaries (Zappfe and Clogg, 1945) [6].

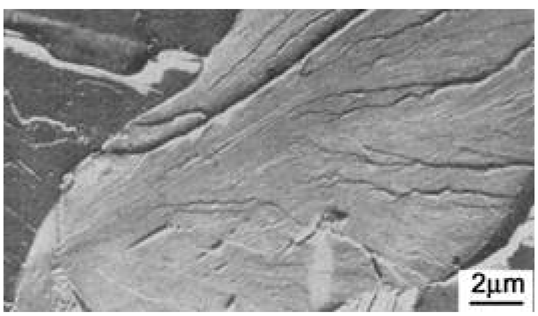

Figure 3. TEM of replica of fracture surface of a steel (ferrite) produced by impact at -40ºC showing fine river lines (Crussard et al. 1956) [8].

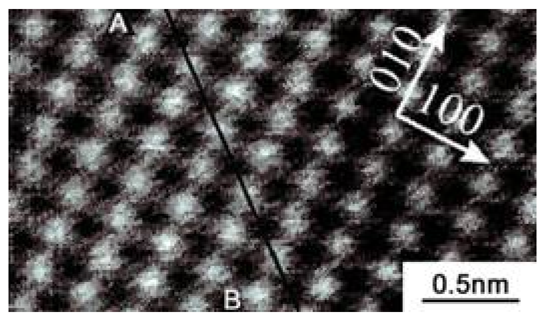

Figure 4. STM of {001} fracture surface of Cr single crystal cleaved in vacuum *(in situ)* at 4.2K showing cubic array of 'atoms' (Kolesnychenko et al., 2001) [11].

Brittle Intergranular Overload Fracture

Many of the brittle fractures observed in early times would often have been intergranular rather than cleavage, due to either the presence of low-melting-point impurity phases or the segregation of impurity atoms at grain boundaries. Intergranular fracture to produce single grains of steel from an overheated bar (Tschernoff, 1878)[3] (Fig. 5) provided an appreciation of the complex shape of metal grains for the first time, and the effect of heat-treatment on grain size was determined from fractographic observations by Brinell in 1885 [3]. Phosphorus impurities as a cause of intergranular embrittlement of steels was first mentioned in 1898, but it was not until the development of Auger Electron Spectroscopy in 1969 that it was demonstrated that fractions of a monolayer of impurities at grain boundaries could produce embrittlement, with the degree of embrittlement increasing with increasing levels of segregation [15,16].

The appearance of intergranular fracture surfaces at high magnifications, like other fracture modes, was first characterised by TEM of replicas from 1956 onwards, and numerous examples were illustrated in Henry and Plateau's classic book "La Microfractographie" in 1967 [10]. Intergranular fracture surfaces resulting from segregation of impurities often appear smooth and featureless (except for particles in some cases), but blocky or wavy steps are sometimes observed since segregated grain boundaries often develop crystallographic facets to minimise the grain-boundary energy (Fig. 6). Embrittlement is generally explained in terms of an atomically brittle 'decohesion' process due to segregation-induced weakening of interatomic bonds across grain-boundaries [e.g. 17]. Two-dimensional grain-boundary phase changes dependent on the degree of segregation and temperature may also be involved – a concept first proposed for temper-embrittlement of steels in 1968 [18, 19]. Significant plasticity is sometimes evident on 'brittle' intergranular fracture surfaces and, hence, crack growth may occur by a very localised plasticity process rather than (or in addition to) decohesion in some cases [19].

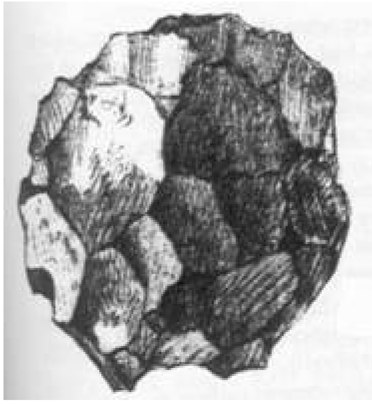

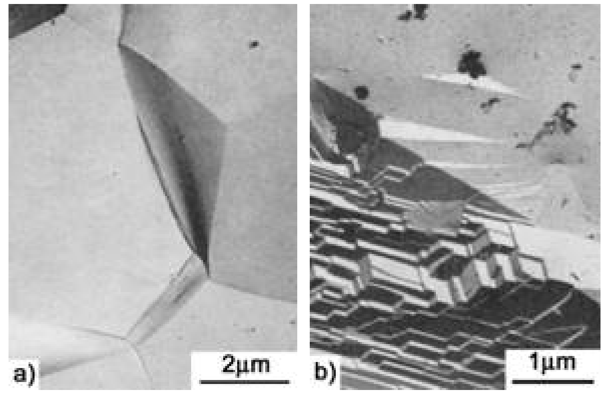

Figure 5. Photograph of a single grain of steel produced by intergranular fracture of an overheated bar (Tschernoff, 1878, reproduced in Smith, 1988 [3]).

Figure 6. TEM of replicas of brittle intergranular fractures at -196ºC in (a) Fe 0.018% O, and (b) commercial-purity Ni with S segregation at boundaries (Henry and Plateau, 1968)[10].

Dimpled Overload Fracture

Réamur's 1722 classification of different sorts of fractures included fibrous ones (and mixtures of fibrous and mirror-like ones), and fibrous fractures were recognised as indicative of good quality (tough) material. Radial markings (steps) diverging from the fibrous fracture origins were first noted by Martens in 1887 (Fig. 7) [2] - an important observation widely used in present-day failure analysis. Fibrous ductile fractures were too rough to be usefully examined by optical microscopy, and significant advances in understanding such fractures by fractographic methods did not occur until they were examined by TEM of replicas, starting in 1956 [8 -10] (Fig. 8) and subsequently by SEM. These TEM and SEM studies, in conjunction with the earlier studies of metallographic sections through cracks, showed that crack growth involved the nucleation, growth, and coalescence of voids, resulting in the formation of dimples (opposing depressions) on both fracture surfaces.

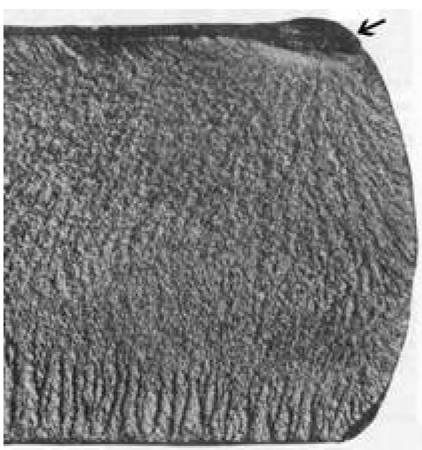

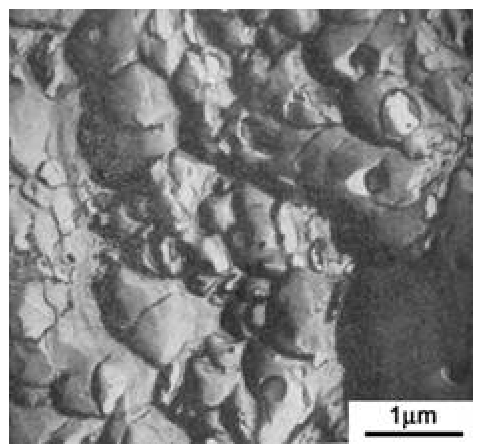

Figure 7. Macroscopic view of fibrous fracture of steel showing steps diverging from crack-initiation sites on the corner of a bar (arrowed) (A. Martens, 1887)(see [2]).

Figure 8. TEM of direct-carbon replica of dimpled fracture surface for a quenched and tempered steel. (Crussard et al. 1956) [8].

Numerous studies [e.g. 9, 20] have shown that the sizes of dimples as well as their shape can vary enormously, with sizes ranging from about 10^{-3}m to about 10^{-7}m, depending on the material, microstructure, temperature, stress-state, and other variables. The size and spacing of second-phase particles are particularly important since voids are initiated preferentially at particles in most materials, although particles are not essential since voids can be initiated at slip-band intersections (and intersections of slip bands with grain boundaries) and at dislocation-cell walls. The shapes of dimples on opposing fracture surfaces are similar (and equi-axed) when fracture occurs locally due to tensile stresses. However, dimple shapes can be quite different on opposite surfaces when fracture involves tearing or shear stresses. Parabolic 'tear dimples' or 'shear dimples' pointing in the same or opposite directions on opposite fracture surfaces, respectively, are then observed. Dimples can also become stretched due to plasticity just behind crack tips, and the extent of stretching can differ on opposite fracture surfaces [9].

In precipitation-hardened materials, grain-boundary precipitates (GBP) and precipitate-free zones (PFZ) adjacent to grain boundaries are often present so that strains are localised within PFZ and voids are nucleated around GBP. Dimpled intergranular fracture surfaces are therefore produced, as described by Ryder and Smale in 1963 [21] and investigated further in the late 1960's by one of the present authors (Fig. 9) [22]. In some cases, particularly when PFZ are narrow and GBP are closely spaced, bright reflective intergranular facets are observed macroscopically, and dimples are sometimes difficult to resolve even using TEM [23]. Fractures in some hcp metals with a limited number of easily activated slip systems, such as magnesium and titanium alloys (especially those with high oxygen levels), are macroscopically brittle, but fracture surfaces are microscopically covered by elongated dimples (termed flutes) (Fig 10) [23, 24]. The cusps of the flutes sometimes form river patterns, and small, relatively equiaxed dimples are sometimes observed within flutes. The formation of flutes involves void nucleation predominantly along slip-band intersections (or slip-band/grain-boundary intersections) so that tubular voids are produced that subsequently coalesce by slip on a single system. Dimples are also observed on macroscopically brittle, 'cleavage-like' fractures in some bcc and fcc materials (Fig. 11)[23, 25]. Further work is required to fully understand the reason why dimpled, cleavage-like fractures sometimes occur, but a possible explanation is that crack growth occurs predominantly by a dislocation-emission (alternate-slip) process that facilitates coalescence of cracks and voids – whereas ductile crack growth probably occurs predominantly by egress of dislocations around crack/void tips [23].

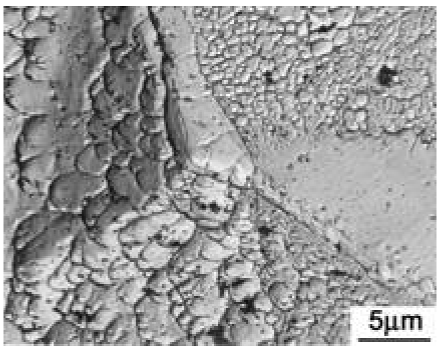

Figure 9. TEM of replica of dimpled intergranular fracture in a peak-aged Al-Zn-Mg alloy (Lynch, 1969) [22].

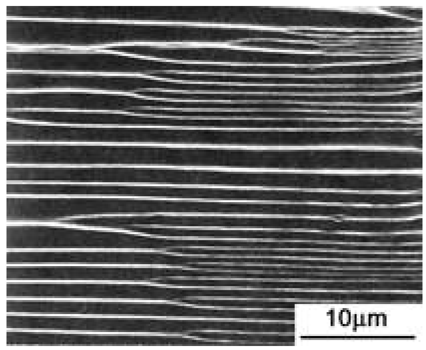

Figure 10. SEM showing flutes on fracture surface of a Ti-O alloy (Meyn and Brooks, 1979) [24].

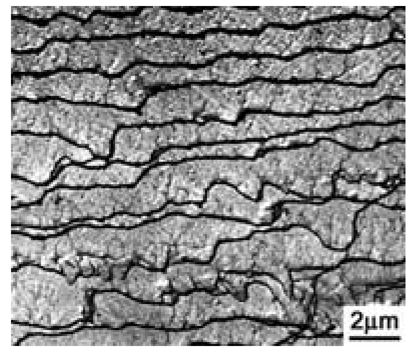

Figure 11. TEM of a dimpled cleavage-like fracture in a bcc Ti-Mn alloy (Williams et al. 1969) [25].

Fatigue Fractures

Fatigue fracture surfaces were first sketched in the early 1840's, with Glynn [26] describing a railway-axle failure having a smooth, cleaved ('crystalline') appearance with blue/purple tints around the periphery and a fibrous appearance in the centre. These fracture-surface observations led some early investigators to conclude that vibration resulted in crystallisation of metals, whereas others correctly maintained that the appearance of fractures depended on the mode of failure. Macroscopically visible 'conchoidal' markings (also called 'beach markings' etc.) on fatigue fracture surfaces would probably have been observed for failures of components in the mid-to-late 1800's, but the first photographs and description as crack-front markings that the authors can find are in Gough's 1926 book 'The Fatigue of Metals' [27] (Fig. 12(a)). An essentially correct explanation for these markings was possibly first proposed by Cazaud [28] in his 1948 book on 'Fatigue of Metals', in which there are a number of examples of fatigue fracture surfaces with progression markings (Fig. 12(b)). Thus, Cazaud suggested that (variable) plastic deformation and work-hardening around cracks resulted in their momentary deflection.

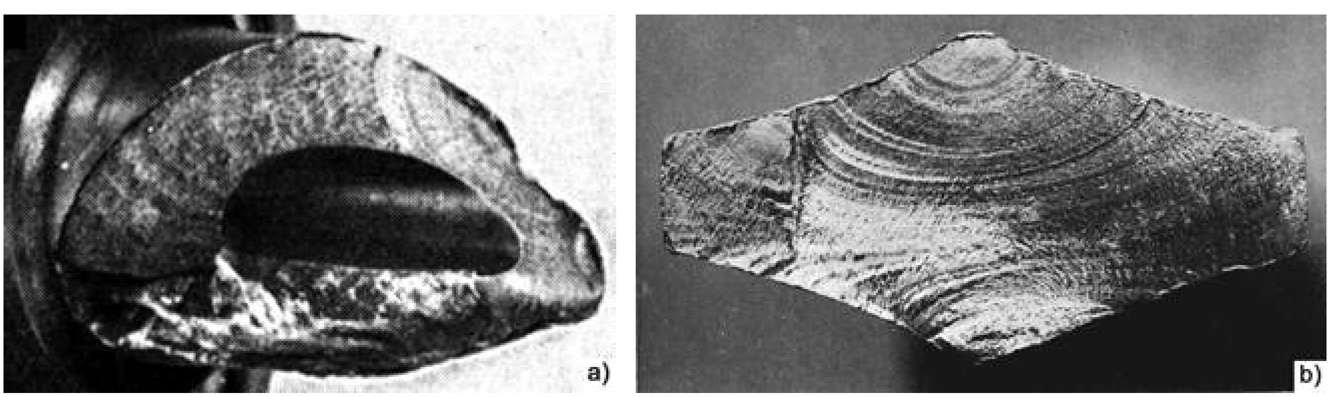

Figure 12. Macroscopic appearance of early fatigue failures showing 'conchoidal' progression markings : (a) for a propeller shaft (Gough, 1926) [27] and (b) for an unidentified component (Cazaud, 1948) [28] (Exact scales are not known).

Microscopic striations on fatigue fracture surfaces (examined by optical microscopy) were first reported in 1950 for an aluminium alloy tested in air by Zappfe and Worden [29], who thought that the markings were associated with some underlying 'cellular structure' of the material. Given that similar macroscopic markings had previously been identified as crack-front markings, it now seems surprising that microscopic striations were not immediately recognised as such, but it was not until 1956 that Crussard [30] realised that this was the case. Crussard initially thought that each striation was produced by about ten stress cycles, then later suggested that each striation was produced by several stress cycles at the very most. Forsyth [31] was probably the first to suggest (in 1957) that each striation was produced by one cycle of stress, and this was demonstrated convincingly by Ryder [32] in 1958 using simple programmed-loading tests and optical microscopy of fracture surfaces (Fig 13(a)). Subsequent fractographic studies in the 1960's and 70's were carried out using TEM [e.g.33,34] (Fig. 13 (b,c)) and these studies, along with metallographic sectioning, TEM of thin foils beneath fracture surfaces, and other techniques, established that striation formation involved crack advance and blunting by slip processes during loading followed by crack-tip re-sharpening (during unloading) involving deformation of part of the surface produced during loading. Faceted, crystallographic, 'stage-II' fractures approximately parallel to {100} or {110} planes at low-to-intermediate ΔK can best be explained by an alternate-slip (e.g. [35], [36]) (or alternate-shear [37]) process on symmetrically orientated planes intersecting crack tips rather than, as sometimes suggested [e.g. 38], by a process involving cleavage.

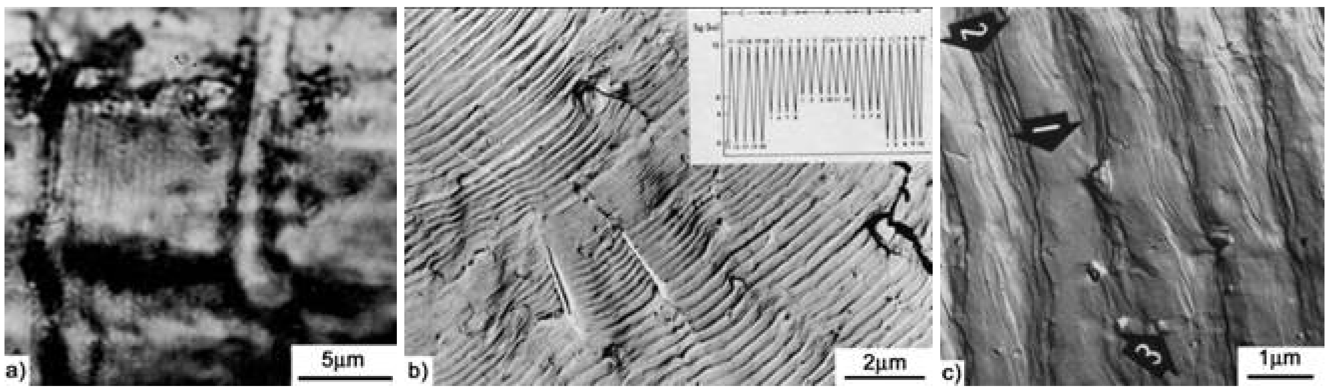

Figure 13. Fatigue striations on fracture surfaces of Al alloys tested in air: (a) optical micrograph showing 18 small striations between larger ones produced by underloads after every 18 constant-amplitude cycles, (Ryder, 1958) [32], (b) TEM of replica showing correspondence between striation spacings and loading programme (inset) (1967)[33], and (c) TEM of replica showing smooth region (1), a rumpled region (2) produced during unloading, and small stretched dimples (3) (1968) [34].

The one-to-one correlation between number of striations and number of stress cycles established by Ryder was later found to hold only at 'intermediate' ΔK values. At low ΔK, every stress cycle does not produce a striation, and there is an increasing discrepancy between striation spacing and macroscopic crack-growth rates with decreasing ΔK, with striation spacings being about the same (80-300nm) for many materials over a range of ΔK (Fig. 14) [39, 40, 41]. It is widely assumed that, at low ΔK, each striation is produced by one cycle of stress (as occurs at intermediate ΔK) and that an increasing number of stress cycles is required before a crack-growth/blunting/re-sharpening event occurs as ΔK decreases because a specific dislocation-cell structure, or some other microstructural change or damage, needs to develop ahead of cracks before crack growth can occur. However, it is possible that crack growth occurs on each cycle (along some parts of the crack front), with sufficient blunting and re-sharpening occurring at crack tips to produce a striation only after cracks have advanced by a critical distance equal to, for example, the dislocation-cell size or slip-band spacing [42]. Further work is required to resolve these issues, and also to explain why there is a minimum striation spacing of about 80-300nm in many circumstances when striation spacings in the range 10-30nm can apparently occur in some circumstances [43].

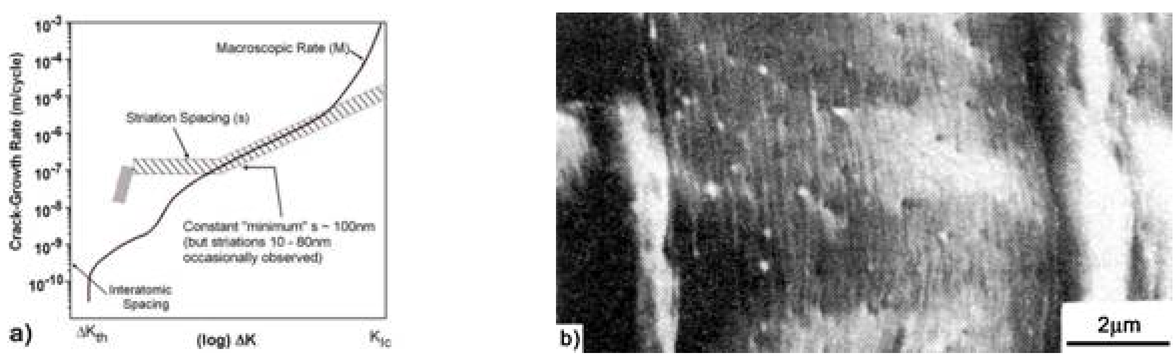

Figure 14. (a) General relationship between macroscopic crack-growth rate, striation spacing, and ΔK for various materials and environments, and (b) SEM of fracture surface of a 2024-T3 Al alloy after fatigue in air with overloads after every 100 cycles. Only forty small striations (~180nm spacing) are present between the larger striations produced by the overloads [41].

Liquid-Metal Embrittlement (LME)

The first observations of LME fracture surfaces reported in the modern literature may well have been in 1875 when Johnson [44] mentioned the embrittlement of zinc by mercury and of iron by zinc, and noted that fracture surfaces for the latter were a blue-grey colour. The first detailed TEM studies of 'brittle' intergranular and cleavage-like fractures, which are produced by LME in normally ductile materials, were carried out by Beachem [9] and others in the mid to late 1960's (Fig. 15(a)). In the 1970's and 80's, metallographic and TEM/SEM fractographic observations of Al, Fe, Ni, Mg, and other materials tested in a variety of liquid metals by Lynch [45, 46] showed that intergranular and cleavage-like fractures were often associated with considerable localised slip on planes intersecting crack tips and that fracture surfaces were sometimes dimpled. For high-strength steels embrittled by liquid mercury, dimples (on transgranular or intergranular facets depending on the steel heat-treatment) appeared much shallower than those produced by overload in air (Fig. 15 (b,c)).

Since there is usually no time or tendency for reactions other than adsorption at crack tips during rapid cracking in liquid-metal environments, Lynch [45] proposed that adsorption facilitated the emission of dislocations from crack tips, thereby promoting the coalescence of cracks with voids formed in the plastic zone ahead of cracks – a process that involves much smaller strains than in inert environments where predominantly egress of dislocations probably occurs. For LME fracture surfaces that are apparently featureless, even when high-resolution techniques are used, it is not clear whether adsorption-induced decohesion occurs, as originally proposed by Westwood et al. in 1967 [47], or whether an adsorption-induced dislocation-emission (AIDE)/void-coalescence process occurs on such a localised scale that dimples are not resolved on fracture surfaces.

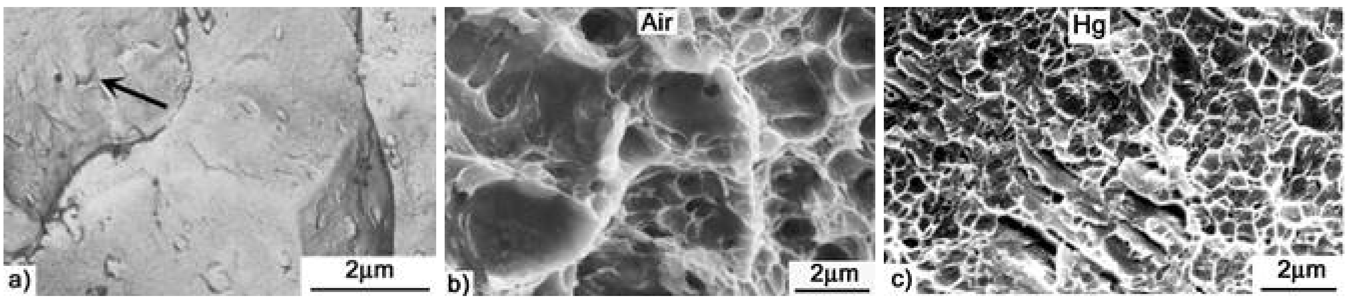

Figure 15. (a) TEM of fracture surface of 2024-T3 Al alloy embrittled by mercury showing intergranular facets with some small dimples (arrowed) (Beachem, 1968) [9], and (b, c) SEM of fracture surfaces of D6aC steel showing large, deep dimples containing smaller dimples after fracture in air, and small, shallow dimples after fracture in mercury (Lynch, 1988) [45].

Hydrogen Embrittlement (HE)

The presence of hydrogen in steels resulted in many failures in the early 20th century, and macroscopic observations of fracture surfaces showed internal 'flakes' or 'fisheyes', with a faceted intergranular or cleavage-like appearance (Fig. 16) [48]. The first detailed fractographic observations of HE (using TEM of replicas) were carried out in the 1960's, and showed that 'brittle' intergranular and 'cleavage' facets exhibited tear ridges and patches of dimples (Fig. 17) [49], and it was generally accepted that HE occurred by a hydrogen-enhanced decohesion (HEDE) mechanism [50]. However, fractographic studies for sub-critical cracking of high-strength steel in hydrogen gas (1 atmos.) by Beachem [51] in 1972 showed that fracture surfaces were completely dimpled at high K levels (Fig. 18). Beachem therefore proposed that solute hydrogen, localized in the plastic zone ahead of cracks, facilitated dislocation activity and thereby promoted crack growth by a localised microvoid-coalescence process – a highly controversial idea at the time.

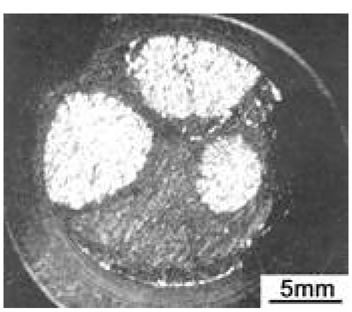

Figure 16. Macroscopic appearance of fracture surface of a notched steel tensile specimen showing 'snowflakes' due to internal hydrogen (1941) [48].

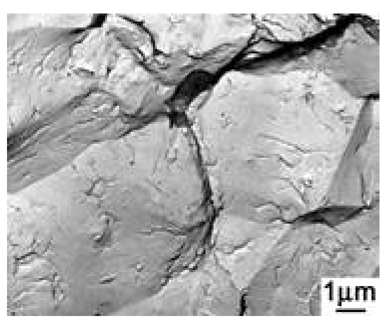

Figure 17. TEM of replica of fracture surface of a H-charged, high-strength 4340 steel showing brittle intergranular facets with tear ridges (1965) [49].

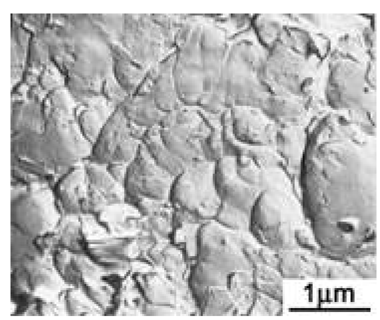

Figure 18. TEM of fracture surface of 4340 steel after sub-critical cracking in H_2 gas resulting in completely dimpled appearance (1972) [51].

Extensive fractographic studies by Lynch (1977-) [45, 46] supported Beachem's view that hydrogen-assisted cracking (in non-hydride forming materials) occurred by a localised-slip process but, partly on the basis of remarkable similarities in the fracture-surface appearances produced by HE and adsorption-induced LME in some materials (Fig. 19), Lynch proposed that adsorbed hydrogen rather than solute hydrogen was responsible. Lynch suggested that cracking occurred by an adsorption-induced dislocation-emission (AIDE) mechanism whereby 'adsorbed' hydrogen (on the crack-tip surface and in the first few atomic layers beneath the surface) weakened interatomic bonds and thereby facilitated the emission of dislocations from crack tips. Fractographic observations that supported Beachem's and Lynch's view that hydrogen-assisted cracking generally occurred by localised-slip processes were subsequently made by Birnbaum and co-workers [52] who, like Beachem, suggested that solute-hydrogen/dislocation interactions were responsible. However, their (solute) hydrogen-enhanced localised-plasticity (HELP) mechanism was largely based on *in-situ* TEM observations of thin foils stressed in hydrogen atmospheres rather than on fractographic observations, and it is difficult to account for some fractographic (and kinetic) aspects of HE by a HELP mechanism, as discussed in detail elsewhere [53]. However, HELP could possibly occur in conjunction with AIDE, and decohesion may also sometimes contribute, for some fracture modes [53].

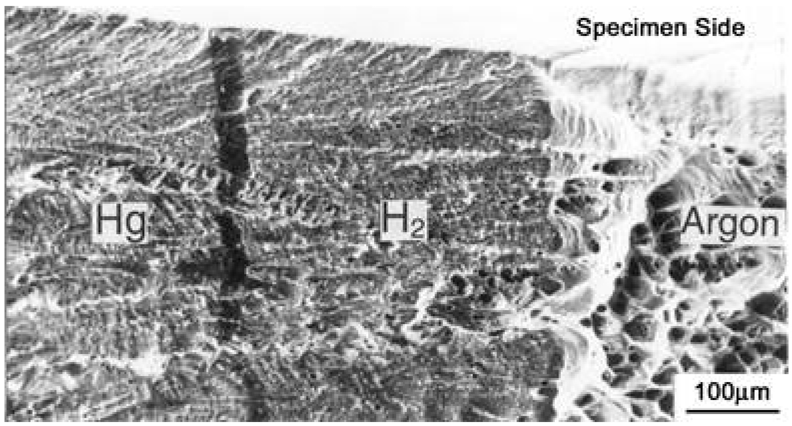

Figure 19. SEM of fracture surface of a notched nickel single crystal cracked first in liquid mercury, then in gaseous hydrogen (1 atmos.), and then in dry argon at 20ºC, showing essentially identical appearance after cracking in mercury and hydrogen. Note that the crack was unloaded slightly to produce a 'striation' marking after (*completely*) evaporating mercury prior to crack growth in hydrogen in order to accurately define the transition position. The fracture-surface appearance in mercury and hydrogen depended on the crystal orientation, but was the same for each orientation (Lynch, 1988) [45].

Other notable fractographic characteristics sometimes observed after HE (in non-hydride forming materials) include cleavage-like {100} <110> fracture surfaces with 'Y-shaped' tear ridges and crack-arrest markings (CAMs) (Fig. 20), both of which match on opposite fracture surfaces [45,54,55]. The tear ridges are probably formed when cracks intersect isolated microvoids ahead of cracks [45, 46] rather than by necking of ligaments left behind crack fronts as has been suggested by some workers [54]. The CAMs result from discontinuous crack growth and intermittent crack-blunting, possibly associated with hydrogen diffusion and accumulation ahead of cracks although other explanations are also possible. Crack growth between the tear ridges and CAMs possibly occurs by an alternate-slip/nano-void coalescence process, resulting in the fine detail observed by TEM of replicas (not resolved by SEM), but an alternate-slip plus decohesion process is also a possibility [54, 55]. For hydride-forming materials, cleavage fractures (or mixtures of cleavage and dimples) are produced as a result of HE when brittle hydrides are formed ahead of cracks [56].

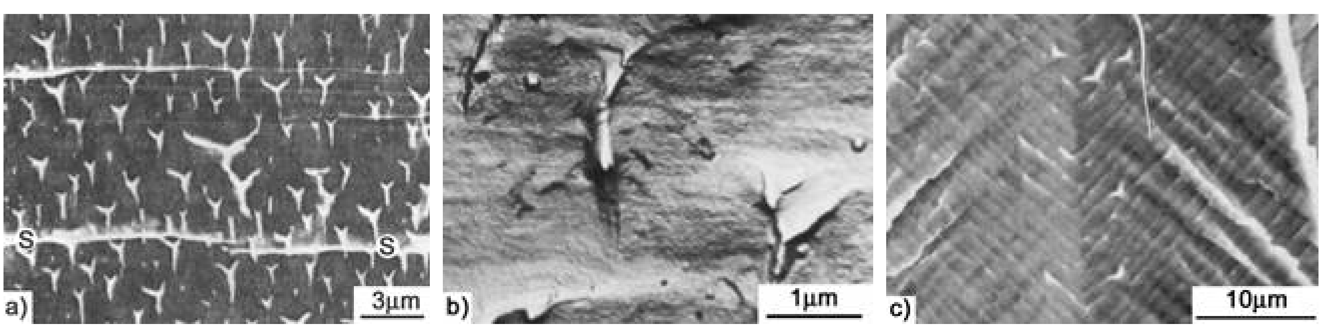

Figure 20. (a) SEM, and (b) TEM of fracture surface of nickel single crystals cracked in H_2 gas showing Y-shaped tear ridges, slip lines (s-s), and fine details between the Y-shaped ridges resolved by TEM, and (c) SEM of fracture surface of Fe-Si single crystal cracked in H_2 gas showing tear ridges and crack-arrest markings (Vehoff et al., 1985 [54], Lynch, 1988 [45], and Chen and Gerberich, 1991 [55], respectively).

Stress-Corrosion Cracking (SCC)

Cracking under sustained stresses in aqueous environments was first mentioned in the 1870's (e.g. [44]). The first recorded industrial problem due to SCC ('season-cracking' of brass cartridge cases in moist ammonia atmospheres) also occurred in the late 1800's but was not recognised as such until 1921 [57]. The first significant fractographic studies of SCC appear to have been carried out in the mid-20th century on Al alloys and stainless steels in particular (where corrosion after fracture sometimes does not obliterate details). These and subsequent studies showed that SCC, like LME and HE, produced 'brittle' intergranular or cleavage-like facets (or both) in normally ductile materials. Intergranular facets were often fairly featureless except for grain-boundary particles and, in some cases, crack-arrest markings (Fig. 21) [58, 59]. Cleavage-like facets (on {100}, {110}, and other low-index crystallographic planes) exhibited fan or feather-like patterns of serrated steps (Fig. 22) [60, 61]. Subsequent work showed that {100} and {110} facets sometimes exhibited fine-scale undulations probably along alternating {111} planes (Fig. 23) [62]. Mechanisms based on stress-assisted directed dissolution, selective-dissolution-vacancy-creep, film-induced cleavage, corrosion-enhanced localized-plasticity, hydrogen-enhanced localized-plasticity (and other hydrogen effects), and adsorption-induced dislocation-emission have all been proposed to account for such fractographic characteristics but there is little general consensus except for a general view that different mechanisms occur in different systems [63].

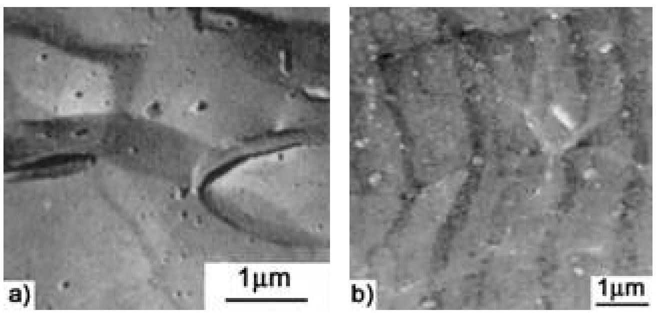

Figure 21. (a) TEM of carbon replica (Forsyth and Ryder, 1961) [58], and (b) SEM (Scamans, 1980) [59] of fracture surfaces for intergranular SCC of 7xxx Al alloys, showing fairly featureless facets and crack-arrest markings.

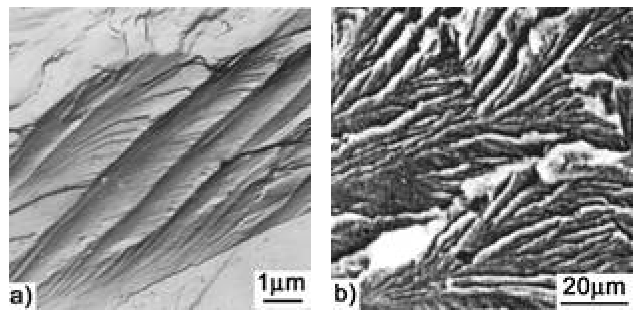

Figure 22 (a) TEM replica (Nielsen, 1969) [60] and (b) SEM (Scully, 1971) [61] of fracture surfaces produced by transgranular SCC of γ-stainless steel, showing feathery pattern of steps.

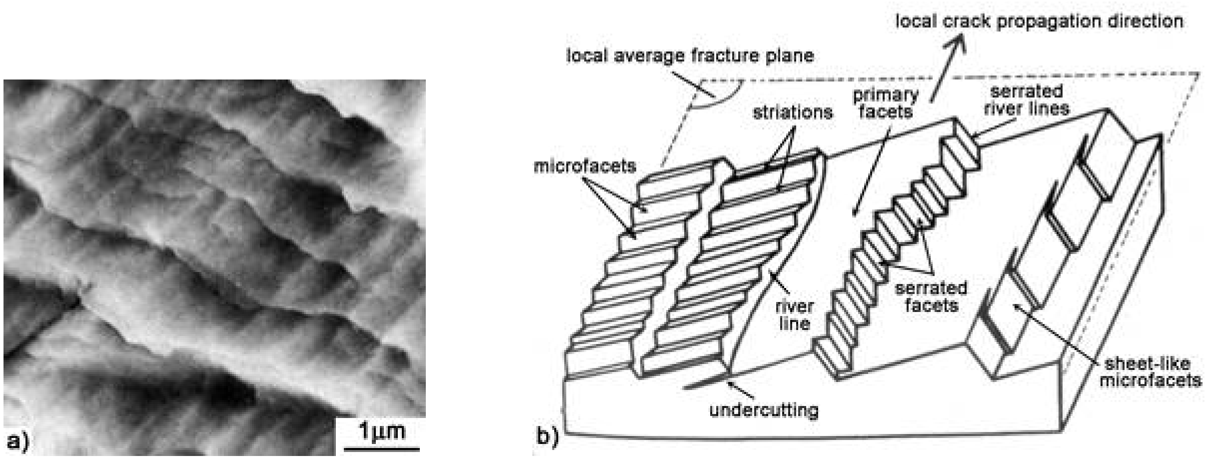

Figure 23. (a) SEM of SCC fracture surface of a stainless steel showing alternating {111} microfacets, and (b) schematic diagram showing typical microfractographic features for transgranular SCC in various fcc materials (Dickson, 1992) [62]. CAMs (not shown) are sometimes observed on primary facets.

Adsorption-based mechanisms of SCC were one of the first proposed, with Uhlig (1959) [64] and Nichols & Rostoker (1963) [65] being early proponents, with the latter drawing particular attention to the general similarities between SCC and adsorption-induced LME. Lynch [45, 46] subsequently showed that SCC and LME in some systems produced essentially identical fracture-surface appearances and crystallography (Fig. 24), supporting a common mechanism. Furthermore, Lynch showed that embrittlement in aqueous environments could occur at very high crack velocities in some circumstances (especially under dynamic loading), supporting an 'adsorbed' hydrogen mechanism. Lynch and others have also suggested that intergranular and cleavage-like SCC fracture surfaces on a very fine scale are sometimes dimpled (Fig. 25) [45 46] (with dimples often resolved by TEM of replicas shadowed at low angles and not by SEM and, hence, subject to some debate regarding whether or not the fine details observed are due to a nanovoid-coalescence process). Further discussion regarding such issues and mechanisms of SCC in general can be found elsewhere [63].

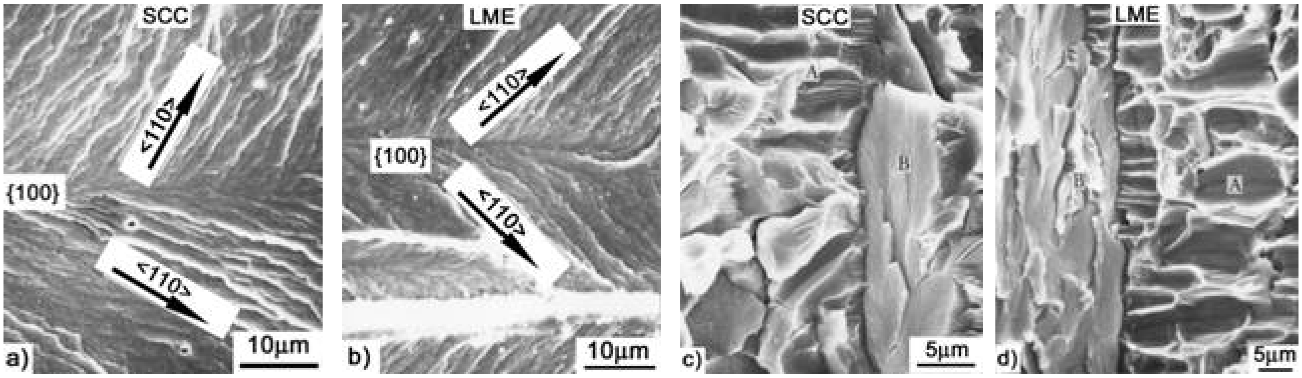

Figure 24. SEM of essentially identical surfaces produced by SCC and LME in (a,b) β-brass showing cleavage-like appearance with herringbone pattern of steps, and (c,d) Ti6Al4V showing fluted areas (A), and cleavage-like {0001} facets (B). (Lynch, 1988) [45, 46].

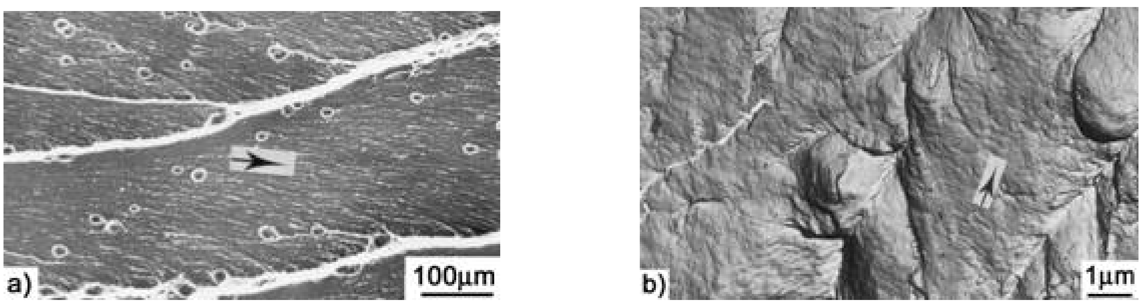

Figure 25. (a) SEM, and (b) TEM of replica of cleavage-like {100} <110> fracture surface of overaged Al-Zn-Mg single crystal cracked rapidly (~10mm/s) in water, showing steps, tear ridges, isolated large dimples, and very small dimples. (Lynch, 1988) [45, 46]. Arrows indicate local crack-growth directions.

Corrosion Fatigue

Corrosion fatigue was first reported by Haigh in 1917 [66], but it was not until the early 1960's that detailed optical and TEM fractography was carried out. These observations showed that 'brittle' striations on cleavage-like and intergranular facets were produced by fatigue in aqueous environments – as opposed to 'ductile' striations produced by fatigue in air (Fig. 26 (a,b)) [67, 68]. Comparisons of fatigue in air and vacuum were also made in the late 1960's [69] showing that the well-defined ductile striations produced in air were often not present after fatigue in vacuum, where fracture surfaces had a rumpled appearance (Fig. 26(c)). The absence of an oxide film at crack tips in vacuum probably results in more blunting during loading, and more slip behind crack tips during loading, than in air thereby producing the rumpled appearance. For corrosion fatigue, studies showed that changes in cyclic frequency or environmental conditions, such as electrochemical potential, solution-composition, or temperature, or changes from embrittling to inert environments (or vice versa), during fatigue generally produced *abrupt* transitions from brittle to ductile striations (or vice versa) (Fig. 26(b)), suggesting that crack-growth processes were controlled by environmental interactions at (or very close to) crack tips, but with precise mechanisms subject to the same controversies as for HE and SCC.

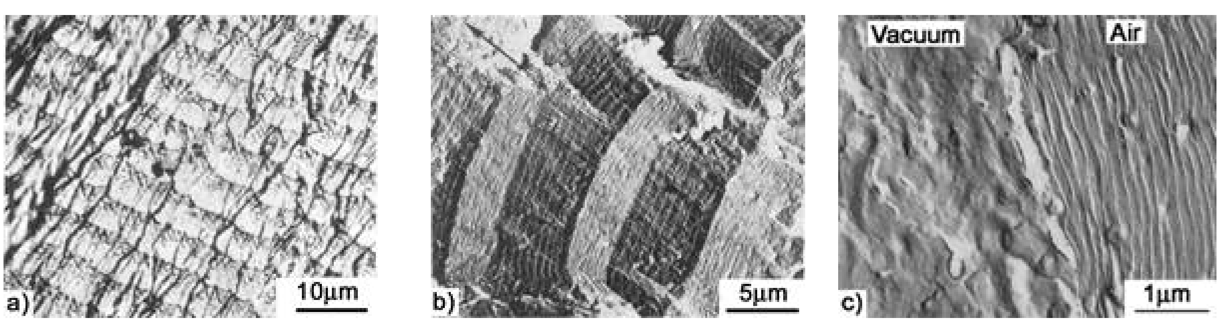

Figure 26. Fatigue fracture surfaces in Al alloys (a) optical micrograph showing brittle striations (Forsyth, 1961) [67] , (b) TEM of replica showing alternate bands of ductile and brittle striations corresponding to cathodic and anodic potentials in sea water, respectively (Pelloux, 1969) [68], and (c) TEM replica showing absence of well-defined striations in vacuum (Meyn, 1969) [69].

Conclusions

There is no doubt that fractography has made a pre-eminent contribution to understanding various modes of fracture (not all of which are covered by this brief overview of its history). The development of high-resolution TEM replica fractography 50 years ago was, of course, of paramount importance. TEM fractography is now rarely used – having been replaced by field-emission SEM and, to a much lesser extent by atomic-force-microscopy (AFM) and scanning tunnelling microscopy (STM), for resolving fine-scale topography. In the authors' opinion, TEM fractography still has a place along with these other techniques in getting a full appreciation of fine-scale fracture surface topography, especially for shallow features on microscopically flat facets. Very small, shallow features can probably be more clearly resolved by TEM of replicas than by FESEM providing that replicas are properly shadowed at low angles (~10º) and examined at low kV (60-80) and high tilt angles (30-45º). In this regard, it would be interesting to compare the *same areas* of such fracture surfaces using all the above techniques.

Despite the advances in understanding various modes of fracture, there are still many outstanding issues that need to be addressed using fractography and other methods. Unresolved questions include (i) why there is such a strong preference for certain crystallographic planes and directions (which vary from one material to another and depend on fracture mode) for brittle and quasi-brittle fractures, (ii) what is the minimum scale for localized-plasticity/void-coalescence processes, (iii) why is there often a minimum fatigue-striation spacing below a certain ΔK for a wide range of materials and environments, and (iv) what are the mechanisms and rate-controlling processes for the various types of environmentally assisted cracking.

References

1 Phillips A., "An Introduction to Crystallography", 3rd edition, Longmans, (1963) and references therein.
2 ASM Handbook 9th Edition, Fractography, ASM, **12**, (1987) and references therein.
3 Smith, C. S., "A History of Metallography", MIT Press (1988) and references therein.
4. Stead, J. E., "The Crystalline Structure of Iron and Steel", Iron and Steel Inst., 145-205 (1898).
5 Zapffe, C. A., Moore, G. A., "A Micrographic Study of the Cleavage of Hydrogenised Ferrite", Trans. of the AIME, **154**, 335-359 (1943).
6 Zapffe, C. A., and Clogg, M. Jr., "Fractography – A New Tool for Metallurgical Research", Trans. ASM, **34**, 71-107 (1945).
7 Hull, D., and Beardmore, P., "Velocity of Cleavage Cracks in Tungsten", Int. J. of Fracture Mechanics, **2,** 468-487 (1966).
8 Crussard, C., Borione, R., Plateau, J., Morillon, Y., and Maratray, F., "A Study of Impact Tests and the Mechanism of Brittle Fracture", Journal Iron and Steel Inst., **183**, 146-177 (1956).
9 Beachem, C. D., "Microscopic Fracture Processes" in Fracture, An Advanced Treatise, Microscopic and Macroscopic Fundamentals, Ed. Liebowitz, H., Academic Press, New York, **1**, 1968.
10 Henry, G., and Plateau, J., "La Microfractographie", Editions Metaux, France, 1968.
11 Kolesnychenko, O. Yu., de Kort, R., and van Kempen, H., "Atomically Flat Ultra-Clean Cr (001) Surfaces Produced by Cleavage of a Single Crystal: Scanning Tunneling Microscopy and Spectroscopy Study", Surface Science, **490**, L573-L578 (2001).
12 Griffith, A. A., "The Phenomena of Rupture and Flow in Solids", Phil. Trans. R. Soc. A, **221A,** 163-198 (1921).
13 Reidle, J., Gumbsch, P., and Fishmeister, H. F., "Cleavage Anisotropy in Tungsten Single Crystals", Physical Review Letters, **76**, 3594-3597 (1996).
14 Knott, J. F., "Micro-mechanisms of Fracture and the Fracture Toughness of Engineering Alloys", Fracture 1977, Ed. Taplin, D. M. R., University of Waterloo Press, Canada, ICF4, **1**, 61-92 (1977).
15 Palmberg, P.W., and Marcus, H. L., "An Auger Spectroscopic Analysis of the Extent of Grain Boundary Segregation", Trans. ASM, **62**, 1016-1018 (1969).
16 Stein, D. F., Joshi, A., LaForce, R. P., "Studies Utilising Auger Electron Emission Spectroscopy on Temper Embrittlement in Low Alloy Steels", Trans. of the ASM, **62**, 776-783 (1969).
17 Briant, C. L., and Banerji, S. K., "Intergranular Failure in Steel: The Role of Grain-Boundary Composition", International Metals Reviews, Review 232, no. 4, 164-199 (1978).
18 Hart, E. W., "Two Dimensional Phase Transformations in Grain Boundaries", Scripta metall., **2**, 179-, (1968).
19 Lynch, S. P., Muddle, B. C., and Pasang, T., "Mechanisms of Brittle Intergranular Fracture in Al-Li alloys and Comparison with other Alloys", Philos. Mag. A, **82**, 3361-3373 (2002).
20 Van Stone, R. H., Cox, T. B., Low, J. R. Jr, and Psioda, J. A., "Microstructural Aspects of Fracture by Dimpled Rupture", Int. Metals Reviews, **30**,157-178 (1985).
21 Ryder, D. A., and Smale, A. C., "A Metallographic Study of Tensile Fractures in Aluminium-Copper and Aluminium-Copper-Zinc-Magnesium Alloys", in Fracture of Solids, Ed. Drucker, D.C., and Gilman, J. J., Interscience Pub. London, 237-259 (1963).
22 Lynch, S. P., "The influence of Microstructure on the Fatigue and Tensile-Deformation and Fracture Characteristics of Aluminium-Zinc-Magnesium Alloys", PhD. Thesis, University of Manchester, (1969).
23 Lynch, S. P., "Ductile and Brittle Crack Growth: Fractography, Mechanisms and Criteria", Mater. Forum, **11**, 268-283 (1988).

24 Meyn, D. A., and Brooks, E. J., “Microstructural Origin of Flutes and Their Use in Distinguishing Striationless Fatigue from Stress-Corrosion Cracking in Titanium Alloys”, in Fractography and Materials Science, ASTM STP 733, Ed. Gilbertson, L. N., and Zipp, R. D., 5-31 (1981).
25 Williams, J. C., Boyer, R. R., and Blackburn, M. J., “The Influence of Microstructure on the Fracture Topography of Titanium Alloys”, in Electron Microfractography, ASTM STP 453, (1969).
26 Glynn, J., “On the Causes of Fracture of the Axles of Railway Carriages" Minutes of Proceedings of the Institute of Civil Engineers, London, **3**, 202-203 (1844).
27 Gough, H. J., “The Fatigue of Metals”, Ernest Benn Ltd., London, (1926).
28 Cazaud, R., “Fatigue of Metals” (1948) Translated by Fenner, A. J., Chapman & Hall, Ltd., London, (1953).
29 Zapffe, C. A., and Worden, C. O., “Fractographic Registrations of Fatigue”, Trans. of the ASM, **43**, 958-969 (1951).
30 Crussard, R., Int. Conf. on Fatigue of Metals, Inst. of Mech. Eng., 748 (1956).
31 Forsyth, P. J. E., “The Application of ‘Fractography’ to Fatigue Failure Investigations”, Technical Note No: MET 257, Royal Aircraft Establishment, Farnborough, U.K., March (1957).
32 Ryder, D. A., “Some Quantitative Information Obtained from the Examination of Fatigue Fracture Surfaces”, Technical Note No: MET 288, Royal Aircraft Establishment, Farnborough, UK, Sept (1958). See also Forsyth, P. J. E., and Ryder, D. A., “Some Results Derived from the Microscopic Examination of Crack Surfaces”, Aircraft Eng., 96-99 (1960).
33 McMillan, J. C., and Pelloux, R. M. N., “Fatigue Crack Propagation under Programmed and Random Loads”, in Fatigue Crack Propagation, ASTM STP 415, 505-535 (1967).
34 Meyn, D. A., “Observations on Micromechanisms of Fatigue-Crack Propagation in 2024 Aluminum”, Trans. of the ASM, **61**, 42-51 (1968).
35 Pelloux, R. M. N., “Crack Extension by Alternating Shear”, Engineering Fracture Mechanics, **1**, 697-704 (1970).
36 Garrett, G. C., and Knott, J. F., “Crystallographic Fatigue Crack Growth in Aluminium Alloys”, Acta metall., **23**, 841-848 (1975).
37 Rieux, P., Driver, J., and Rieu, J., “Fatigue Crack Propagation in Austenitic Stainless Steel Single Crystals”, Acta metal., **27,** 145-153 (1979).
38 Nix, K. J., and Flower, H. M., “The Micromechanisms of Fatigue Crack Growth in a Commercial Al-Zn-Mg-Cu Alloy”, Acta metall., **30**, 1549-1559 (1982).
39 Davidson, D. L., and Lankford, J., “Fatigue Crack Growth in Metals and Alloys: Mechanisms and Micromechanisms”, International Materials Reviews, **37**, 45-76 (1992).
40 Grinberg, N. M., “Stage II Fatigue Crack Growth”, Int. J. Fatigue, **6,** 229-242 (1984).
41 Kiese, J., Gysler, A., and Lütjering, G., “Fatigue Crack Propagation Mechanisms in Al-Alloys under Variable Amplitude Loading” in Fatigue 90, Ed. Kitagawam, H., and Tanaka, T., 1523-1528 (1990).
42 Riemelmoser, F. O., Pippan, R., and Stüwe, H. P., “An Argument for a Cycle-by-Cycle Propagation of Fatigue Cracks at Small Stress Intensity Ranges”, Acta. Mater., **46**, 1793-1799 (1998).
43 Broek, D., “Some Contributions of Electron Fractography to the Theory of Fracture”, International Metallurgical Reviews, **19**, 135-182 (1974).
44 Johnson, W.H., “On the Remarkable Changes Produced in Iron and Steel by the Action of Hydrogen and Acids” Proc. Royal Society of London, **23**, 168-180 (1874-75).
45 Lynch, S. P., ‘Environmentally Assisted Cracking: Overview of Evidence for an Adsorption-Induced Localised-Slip Process’, Acta metall., **36**, 2639-2661 (1988), and references therein.
46 Lynch, S. P., “Metallographic Contributions to Understanding Mechanisms of Environmentally Assisted Cracking”, Metallography, **23**, 147-171 (1989).
47 Westwood, A.R.C., Preece, C.M., and Kamdar, M.H., “Application of a Crack Propagation Criterion to LME: Cleavage of Aluminium Monocrystals in Liquid Gallium”, Trans. ASM, **60,** 211-213 (1967).
48 Zapffe, C. A., and Sims, C. E., “Hydrogen Embrittlement, Internal Stress and Defects in Steel”, Trans AIME., **145**, 225-261, (1941).
49 Phillips, A., Kerlins, V., and Whiteson, B. V., Electron Fractography Handbook, MCIC-HB-8. Metals and Ceramics Info. Ctr., Columbus, OH (1976) originally published as Report AFML-TR-64-416, Air Force Systems Command, Wright-Patterson AFB, OH, Jan (1965).
50 Troiano, A. R., ‘The Role of Hydrogen and Other Interstitials in the Mechanical Behavior of Metals’ Trans. ASM, **52**, 54-80 (1960).
51 Beachem, C. D., “A New Model for Hydrogen Assisted Cracking (Hydrogen Embrittlement)”, Metall. Trans. **3**, 437-451 (1972).
52 Birnbaum, H. K., and Sofronis, P., “Hydrogen-Enhanced Localised Plasticity – A Mechanism for Hydrogen - Related Fracture”, Mater. Sci. Eng., **A176**, 191-202 (1994).
53 Lynch, S. P., “Mechanisms of Hydrogen Assisted Cracking – A Review”, in Hydrogen Effects on Materials Behavior and Corrosion Deformation Interactions, Ed. N. R. Moody et al., TMS, 449-466 (2003), and references therein.
54 Vehoff, H., and Klameth, H. -K., “Hydrogen Embrittlement and Trapping at Crack Tips in Ni-Single Crystals”, Acta metall., **33**, 955-962 (1985).
55 Chen, X., and Gerberich, W. W., “The Kinetics and Micromechanics of Hydrogen-Assisted Cracking in Fe-3 Pct Si Single Crystals”, Metallurgical Trans. A, **22A**, 59-70 (1991).

56 Gahr, S., Grossbeck, M. L., and Birnbaum, H. K., “Hydrogen Embrittlement of Nb I - Microscopic Behaviour at Low Temperatures”, Acta metall., **25**, 125-134 (1977).
57 Moore, H., Beckinsale, S., Mallinson, C. E., “The Season Cracking of Brass and Other Copper Alloys”, Journal of the Institute of Metals, **25**, 35-152 (1921).
58 Forsyth, P. J. E., and Ryder, D. A., “Some Results of Examination of Aluminium Alloy Specimen Fracture Surfaces”, Metallurgia, **63**, 117-124 (1961).
59 Scamans, G. M., “Evidence for Crack-Arrest Markings on Intergranular Stress Corrosion Fracture Surfaces in Al-Zn-Mg Alloys”, Metallurgical Trans. A, **11A**, 846-850 (1980).
60 Nielsen, N. A., “Electron Microfractography of Stress-Corrosion Cracking”, in Fundamental Aspects of Stress Corrosion Cracking, Eds. Staehle, R. W., Forty, A. J., and Van Roogen, D., NACE, 308-317 (1969).
61 Scully, J.C., “Fractographic Aspects of Stress Corrosion Cracking”, in “The Theory of Stress Corrosion Cracking in Alloys”, Ed. Scully, J. C., North Atlantic Treaty Organization, Brussels, 127-166 (1971).
62 Dickson, J. I., Shiqiong, Li, Bailon, J. P., and Tromans, D., “The Fractography of Transgranular SCC in FCC Metals: Mechanistic Implications”, Parkins Symposium on Fundamental Aspects of Stress Corrosion Cracking, Ed. Bruemmer, S. M. et al., The Minerals, Metals & Materials Society, 303-322 (1992).
63 “Corrosion-Deformation Interactions”, Second int. Conf. on Corrosion-Deformation Interactions, Ed. Magnin, T., Institute of Materials, France, Nice, (1996). See also, “Hydrogen Effects on Materials Behavior and Corrosion Deformation Interactions”, Proceedings of the Int. Conf. on Hydrogen Effects on Material Behavior and Corrosion Deformation Interactions, Ed. Moody, R. N. et al., TMS, Moran, Wyoming (2002).
64 Uhlig, H., “New Perspectives in the Stress Corrosion Problem”, in Physical Metallurgy of Stress Corrosion Fracture”, Ed. Rhodin, T., Interscience Publ. New York, (1959).
65 Nichols, H., and Rostoker, W., “Analogies between Stress-Corrosion Cracking and Embrittlement by Liquid Metals”, Trans. ASM, **56**, 494-507 (1963).
66 Haigh, B. P., “Experiments on the Fatigue of Brasses”, J. Inst. of Metals, **18**, 55-86 (1917).
67 Forsyth, P. J. E., “A Two Stage Process of Fatigue Crack Growth”, in Proceedings of the Crack Propagation Symposium, Cranfield, **1**, 76-94 (1961).
68 Pelloux, R. M. N., “Corrosion Fatigue Crack Propagation”, in Fracture 1969, Proc. 2nd int. Conf. on Fracture, Brighton, Chapman and Hall, London, 731-744 (1969).
69 Meyn, D. A., “The Nature of Fatigue-Crack Propagation in Air and Vacuum for 2024 Aluminum, Trans. ASM, **61**, 52-61(1968).

General Bibliography

A Phillips, A., Kerlins V., and Whiteson, B. V., “Electron Fractography Handbook”, MCIC-HB-8, Metals and Ceramics Info. Ctr., Columbus, OH (1976) originally published as report AFML-TR-64-416, Air Force Systems Command, Wright-Patterson AFB, OH, Jan (1965).

B “Electron Fractography”, ASTM, STP 436 (1968).

C Henry, G., and Plateau, J., “La Microfractographie”, Editions Metaux, France (1968).

D “Electron Microfractography”, ASTM, STP 453 (1969).

E Ryder, D. A., “The Elements of Fractography”, AGARDograph No. 155, AGARD (Advisory Group for Aerospace Research Development), NATO (1971).

F “Fractography - Microscopic Cracking Processes”, Ed. Beachem, C.D., and Warke, W. R., ASTM, STP 600 (1976).

G Henry, G., and Horstmann, D., “De Ferri Metallographia V”, “Fractography and Microfractography”, Stahleisen Verlag, Düsseldorf, m.b. H., (in English, German, and French) (1979).

H “Fractography and Materials Science”, Ed. Zimmer, G., Gilbertson, L. N., and Zipp, R. D., ASTM, STP 733 (1981).

I “ASM Handbook”, Formerly 9th Edition, Metals Handbook, vol. 12, Fractography, ASM (1987).

J “Fractography of Modern Engineering Materials: Composites and Metals”, Ed. Masters, J. E., Au, J. J., ASTM, STP 948 (1987).

K Hull, D., “Fractography - Observing, Measuring and Interpreting Fracture Surface Topography”, Cambridge Univ. Press (1999).

L Brooks, C.R., and Choudhury, A., “Failure Analysis of Engineering Materials”, McGraw-Hill (2002).